Journal of Highway and Transportation Research and Development
2024, 18(4) : 128−135

Research Article
ISSN 2095−6215
DOI: 10.26599/HTRD.2024.9480042

Degradation analysis of concrete bridge load-bearing capacity based on crack distribution

Zhirong Ma[1, 2*], Xiaoguang Wu[2**], Xingke Chang[3], Jiang Huang[4]

1. *Ankang Public Works Section, China Railway Xi'an Bureau Group Co., Ltd. , Ankang, Shaanxi 725000, China*;
2. *School of Highway, Chang'an University, Xi'an, Shaanxi 710064, China*;
3. *Shanxi Province Expressway Group Limited Liability Company, Taiyuan, Shanxi 030031, China*;
4. *Shanxi Provincial Highway Bureau, Taiyuan, Shanxi 030006, China*

Abstract: In-service reinforced concrete bridges, following prolonged operational periods, frequently undergo alterations in structural integrity and significant deterioration of material properties. As a result, it becomes imperative to evaluate and analyze these bridge structures. This study focuses on a specific in-service concrete bridge and employs finite element simulation analysis to investigate the failure behavior and degradation of load-bearing capacity in concrete beam bridge structures. The research examines the impact of various crack distributions and types, specifically addressing the effects of bending and shear cracks on the failure behavior and degradation of load-bearing capacity in concrete bridge structures. Load simulations are conducted on the bridge, revealing that bending cracks exert a relatively minor influence on the failure mode of the structures. The load-deflection curves demonstrate minimal variation across different crack heights, indicating that the structures do not experience abrupt brittle failure, and their structural performance is largely optimized in this context. Conversely, shear cracks have a pronounced effect on the failure mode of the bridge structures. Notably, when the crack height reaches 0.6h, the load-deflection curve exhibits a significant alteration, leading to brittle failure attributed to shear cracks, thereby indicating that the structural performance is not fully realized. Given that the deformations in cracked bridge structures comprise two components, stiffness reduction formulas are introduced. Utilizing the stiffness reduction formula outlined in the standard (JCT3362—2018) for cracked components, a formula for calculating residual load-bearing capacity is derived. Calculations pertaining to the mid-span section load-bearing capacity of the selected bridge reveal deviations within 5%. This study offers a valuable methodology and reference for assessing the residual load-bearing capacity of reinforced concrete bridges exhibiting crack damage.

Keywords: bridge engineering; degradation of bearing capacity; structural cracks; reduction of stiffness; calculation of residual bearing capacity

1 Introduction

Bridges play a vital role in the national transportation network due to their lightweight and strong spanning capabilities. Reinforced concrete bridges are widely used in China. However, with the extension of their operational lifetimes, many bridges experience structural cracking and aging material properties, leading to varying degrees of harm to the overall integrity and safety of bridge structures. When assessing and analyzing concrete bridges that have been in service for an extended period, the influence of cracks on bridge structures is a major challenge and focal point of analysis. There are numerous uncertain influencing factors. Concrete structural design often relies on certain basic assumptions, such as the assumption that the cross-sectional average strain conforms to the cross-section's assumption of being plane, and it does not consider the tensile strength of cracked concrete in the tensile zone. When analyzing

Received: 26 December 2023; **Revised:** 10 March 2024; **Accepted:** 27 June 2024

[*] *E-mail address*: 1519842045@qq.com

[**] *Corresponding author*: wxgwst.cn@126.com

Translated from *Journal of Highway and Transportation Research and Development* (Chinese, ISSN1002-0268), 2024, 41(8): 154−161.

cracked concrete structures, idealized assumptions and mechanical models are often used, which reduces the impact of cracks on structural behavior. This idealization in the analysis of cracked concrete bridge structures calls for a more realistic approach. Therefore, conducting load-bearing capacity analysis of cracked concrete beam bridge structures is of practical significance for the design, inspection, maintenance, and regular assessment of concrete bridges.

In recent years, both domestic and international scholars have conducted extensive research on the condition of reinforced concrete beam bridge structures after cracking. Sherif [1] established a new relationship by considering the post-cracking strength of concrete and its fracture energy, tensile strength, and ultimate crack width. Castel[2] assumed a nonlinear distribution of strain in reinforcement, concrete strain, and the neutral axis between two continuous bending cracks to calculate the average moment of inertia within macroscopic elements. They developed a finite element model to calculate the overall stiffness of cracked reinforced concrete beams. Ismail[3] developed different FE models to study the trend of stiffness loss in RC beams due to varying degrees of cracking and compared their results with experimental data, showing good agreement. Benakli[4] developed a finite element model capable of simplifying and quickly calculating the nonlinear load-displacement behavior of reinforced concrete structures. They proposed relationships covering the crack phase up to the yield point of the steel based on material properties, reinforcement ratio, and crack width. Domestic scholars, including Zhao[5], considered material nonlinearity and established iterative formats for section equilibrium and expressions for section damage stiffness. However, they assumed that all cracks in the structural bending zone were tensile cracks. Li[6] used a cross-sectional nonlinear full-process research method to obtain the corresponding function between the moment and crack height for the key sections of bridges in a universal diagram. They also established a crack characteristic database. Wang[7] simulated longitudinal cracks based on statistical characteristic parameters of cracks and used a degradation method to model transverse cracks in prestressed concrete box bridge structures. They analyzed the residual load-bearing capacity of cracked prestressed concrete bridges. Li[8] considered three factors: vertical natural frequency, linear stiffness, and width-to-span ratio. They introduced a main beam damage reduction coefficient and used the multivariate nonlinear regression analysis method in MATLAB to fit the coefficient. They compared it with data from load tests on actual bridges. Zhu[9] conducted loading and failure tests on seven prestressed concrete T-beam models. They studied the expansion patterns of crack height, width, and density during the failure process of prestressed T-beam bridges.

Considering the substantial research achievements made by numerous scholars regarding the relationship between the stiffness, load-bearing capacity of cracked concrete bridges, and crack data parameters, this paper focuses on the structural failure of concrete bridge structures. Through the establishment of finite element models for numerical simulation, the study examines the influence of crack morphology on structural load-bearing capacity and failure modes. This research plays a pivotal role in promoting the regular assessment, management, and maintenance decisions for long-serving concrete bridges.

2 Bridge information

This paper selects a bridge constructed on a provincial trunk road in a certain country in the 1980s. The design loads are in accordance with the Highway Bridge Design Code (JTGD60—2015)[10], with a road classification of Highway Class I. The main bridge structure consists of a 2 × 25 m T-beam bridge. Figure 1 illustrates the schematic diagram of the bridge structure, while Figure 2 presents a cross-sectional schematic of the T-beam structure of the bridge.

With the increasing traffic volume and over half a century of service, the bridge has experienced phenomena such as material degradation and structural deterioration.

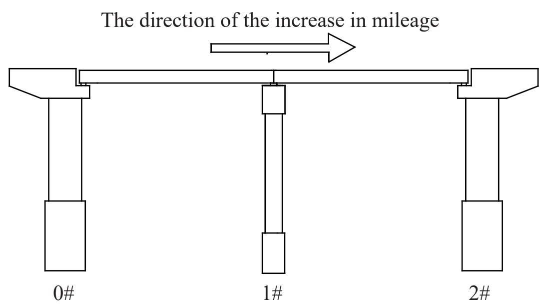

Fig. 1 Schematic diagram of bridge structure

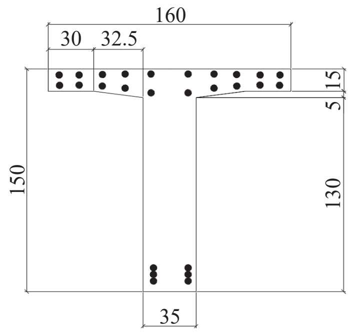

Fig. 2 Cross section of bridge (unit: cm)

In accordance with the (JTG/TH21—2011)[11], the maintenance unit regularly conducts relevant bridge inspections. According to the most recent bridge inspection report, the bridge's deck system exhibits pavement deterioration, cracks, clogged expansion joint slots, localized concrete spalling, and missing guardrails. In the upper structure, the T-beam's bottom concrete is spalling, and there are cracks. In the lower structure, there is detachment of the slope protection hook joint. According to the (JTG/TH21 —2011), the overall technical assessment condition level of the bridge, as shown in Table 1, is categorized as a Class 2 bridge. The presence of cracks in the upper structure poses a safety hazard to the bridge's operation. Building upon previous research by scholars, this study aims to investigate the adverse effects of existing crack morphologies on the structure by establishing Finite Element Analysis (FEA) models. The research will also focus on assessing the impact of the primary structural load-bearing cracks based on field inspection data. As the objective is to explore the influence of cracks on the upper structure, a single 25 m-span upper T-beam structure will be chosen for modeling and analysis.

Table 1 Technical condition evaluation form of the whole bridge

Bridge section	Weights	Technical condition rating	Technical condition rating of the bridge
Superstructure	0.4	2	
Understructure	0.4	2	2
Bridge facade system	0.2	3	

3 Finite element modelling (FEM)

This paper utilized the numerical analysis software DIANA to create a physical model of the bridge. Analyzed the bridge's structural behavior, load-deflection curves, and damage patterns under the influence of various loads. The experimental beam VS-C3, as conducted by Vecchio et al.[12], served as a reference for comparison with our numerical simulation results. Figure 3 illustrates the structural parameters of the VS-C3 beam, while Tables 2 and 3 provide the necessary material parameters for VS-C3. Conducted numerical simulations of the experiment, where a reinforced concrete beam was subjected to static loading until failure. Linear elastic material properties were applied to the steel plates used for loading and support modeling. Interface elements were employed between the steel plates and the concrete beam. These elements increased the applied load incrementally to simulate the displacement of the steel plate until the beam ultimately failed, enabling us to perform a static nonlinear analysis of the beam.

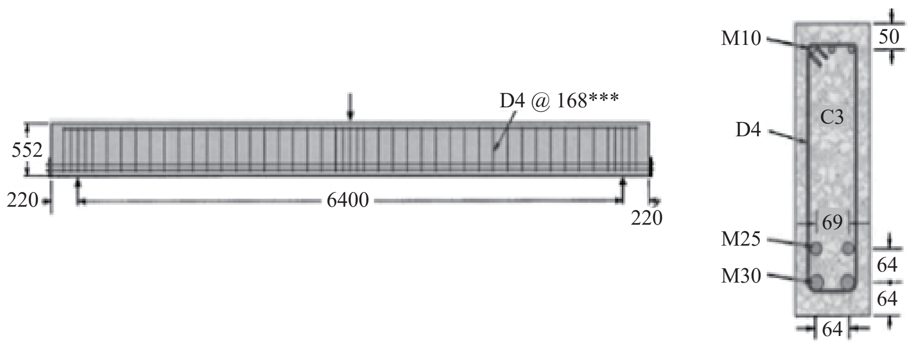

Fig. 3 Structural diagram of VS-C3 beam (unit: mm)

Table 2 Concrete material parameters

Young's modulus	Poisson's ratio	Compressive strength (N/mm^2)	Tensile strength (N/mm^2)
34 300	0.2	43.5	3.13

Table 3 Rebar material parameters

Designation	Diameter (mm)	Yield strength (N/mm^2)	Ultimate strength (N/mm^2)	Ultimate strain	Young's modulus (N/mm^2)
10	11.3	315	460	0.05	200 000
25	25.2	445	680		
30	29.9	436	700		
D4	5.7	600	651		

3.1 Material constitutive mode

In conducting finite element modeling and analysis, the material constitutive relationship plays a crucial role in determining the accuracy of the computational results[13]. In this finite element solid modeling and numerical analysis, to enhance the precision of the simulation results, the concrete constitutive relationship adopted the total strain-crack model, as recommended in the concrete model specification by the International Federation for Structural Concrete (fib). This constitutive relationship can accurately simulate the mechanical behavior and crack distribution throughout the entire process of concrete cracking and failure[14]. The chosen constitutive model exhibits exponential softening during tension and parabolic characteristics during compression. This model describes stress-strain behavior such that loading and unloading follow the same stress-strain path. Additionally, the crack angle continuously changes with stress updates, always perpendicular to the principal tensile stress direction. The total strain rotation crack model ensures the co-axiality of principal strain and stress by continually rotating the principal stress axis. This prevents shear locking issues. Figure 4 illustrates the constitutive relationship of the total strain rotation crack model.

The constitutive relationship for the steel reinforcement adopts the Tresca and Von Mises plasticity criteria. The Tresca model posits that material yields when the maximum shear stress reaches a certain limit, as shown in Equation (1). On the other hand, the Von Mises model considers the influence of intermediate principal stresses on material yield, addressing the computational difficulties arising from the non-smooth yield curve in the Tresca model. It proposes using a yield surface in the shape of a circle that connects the six vertices of the Tresca model's yield conditions. The yield conditions are represented by Equation (2).

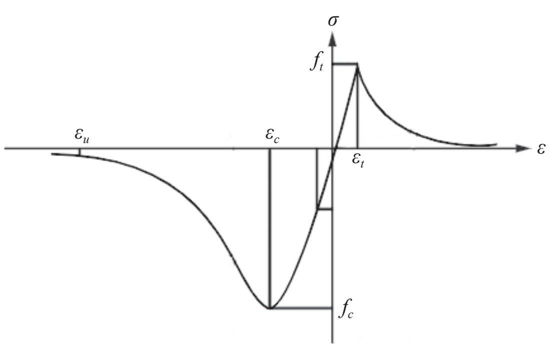

Fig. 4 Constitutive relation diagram of concrete

$$f(\sigma, \kappa) = |\sigma_1 - \sigma_2| - \overline{\sigma}(\kappa), \tag{1}$$

$$f(\sigma,\eta,\kappa)= \sqrt{3J_2}-\overline{\sigma}(\kappa)= \sqrt{\frac{1}{2}(\sigma-\eta)^{\mathrm{T}}P(\sigma-\eta)}-\overline{\sigma}(\kappa). \tag{2}$$

3.2 Model validation

Concrete is modeled using plane stress elements, while hoops and reinforcement are modeled using embedded reinforcement elements. For computational convenience, modeling is performed only on half of the beam based on symmetry. Interface elements are used to model the interaction between the steel plate and concrete, and nonlinear elastic properties are assigned to the interface elements. The finite element model for VS-C3 is depicted in Figure 5.

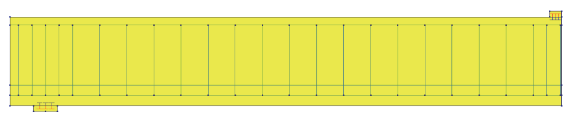

Fig. 5 VS-C3 finite element model diagram

The finite element model was subjected to loading until structural failure occurred, with displacement applied as a simulated load. In the nonlinear analysis, a small displacement increment was applied, with a vertical direction increment of 0.1 mm for deformation. The simulation results were then analyzed, including displacement, support reactions, crack strains, total strains, and stresses. As shown in Figure 6(a), it depicts the simulated structural failure of the finite element model, while Figure 6(b) shows the observed structural failure of experimental beam VS-C3. It can be observed that the concrete near the loaded region was crushed, and the structural failure was caused by bending. The results obtained from the finite element simulation are in good agreement with the experimental observations.

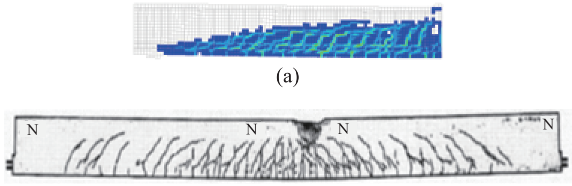

Fig. 6 Simulation and experimental comparison of cracking forms of VS-C3 Beam

The displacement values were obtained by selecting the lowest node at the midspan of the finite element model , and the support reactions were recorded at the support points. The load applied was twice the reaction force, and a load-displacement curve was plotted. As shown in Figure 7, it can be observed that the numerical results closely match the experimental results[12].

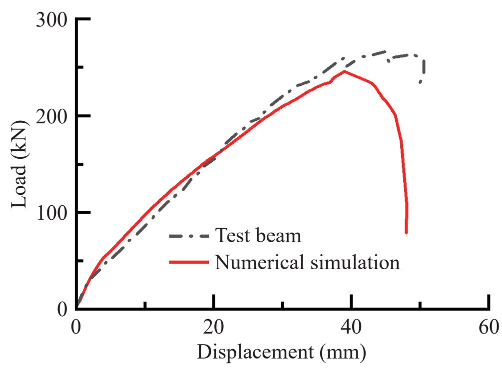

Fig. 7 Simulated load displacement curves

3.3 fracture modeling

Concrete structures often work with cracks due to the material characteristics of concrete. However, as cracks extend, the load-bearing capacity of the structure gradually decreases, especially in concrete bridges[15]. Building upon the experiments conducted by Vecchio and Shim, this paper explores the influence of different forms of structural cracks on the load-bearing capacity of structures. In RC bridge structures, the primary types of load-induced cracks are flexural cracks and shear cracks. Based on the data reported in the bridge inspection reports, both flexural and shear cracks were incorporated into the finite element model[16], as shown in Figure 8.

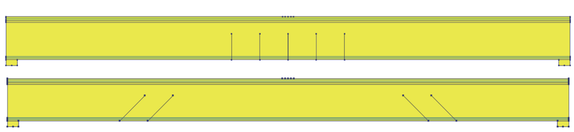

Fig. 8 Schematic of crack location

The crack modeling in this study employs a discrete cracking modeling method, involving discrete crack interfaces that connect the solid elements on both sides. These discrete interfaces define functions relating stress to total relative displacement, crack width, and relative slip of the crack. They act as force connectors between the solid elements on both sides of the crack. The properties of the interface elements are set in a way that they can only withstand compressive forces and will open when subjected to tensile forces at the crack location.

4 Analysis of simulation results

To ensure the representativeness and practical value of the study, the research investigates the impact of shear cracks and flexural cracks on the structural load capacity under different crack heights. Crack heights of 0.2 h, 0.4 h, 0.6 h, and 0.8 h are chosen to conduct numerical analyses of the bridge structure's load capacity under various crack conditions. The analysis includes scenarios where only flexural cracks or only shear cracks are present, and the corresponding results of structural failure are examined.

4.1 Analysis of results under different heights of bending cracks

As shown in Figure 9, when only flexural cracks are present, a three-point bending test simulation is conducted. Under different crack height conditions, load-displacement curves are obtained. It can be observed that with changes in the height of flexural cracks, the structural failure behavior of the beam under gradually increasing load does not show significant variations. There is no sudden brittle failure, and the structure exhibits a certain level of ductility. At the ultimate state, the structure can still accommodate some deformation. It can be concluded that the failure mode of the RC beam under flexural crack conditions is generally flexural failure.

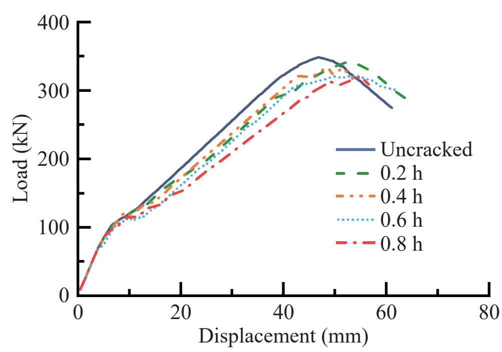

Fig. 9 Load displacement curves (bending crack)

As shown in Figure 10, it illustrates the structural crack pattern and the stress distribution of the steel reinforcement in this scenario. According to the principles of concrete structural design, the bottom longitudinal reinforcement reaches a yielding state under tension in the midspan area, while the top longitudinal reinforcement assists in compression of the midspan portion under load. Additionally, the stirrups at the cracking location assist in tension, and when the structure fails, their own properties are essentially utilized.

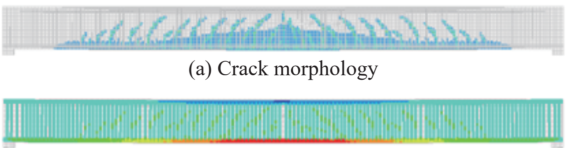

(a) Crack morphology

(b) Reinforcement stress, hoop stress

Fig. 10 Cracks and reinforcement stress diagram (bending crack)

4.2 Analysis of results under different heights of shear cracks

As shown in Figure 11, when only shear cracks are present, simulations were conducted for different crack heights, resulting in load-displacement curves. It can be observed that with increasing shear crack height, the structural failure behavior gradually changes as the load is applied. When the crack height is relatively small, the structural failure of the beam exhibits ductile behavior, When the shear crack height increases, the beam structure suddenly undergoes failure, exhibiting brittle behavior. Additionally, when the shear crack height is relatively high, the deflection at the midspan of the structure under load is also small. This indicates that the RC beam structure experiences brittle failure with minimal deformation in the presence of shear cracks.

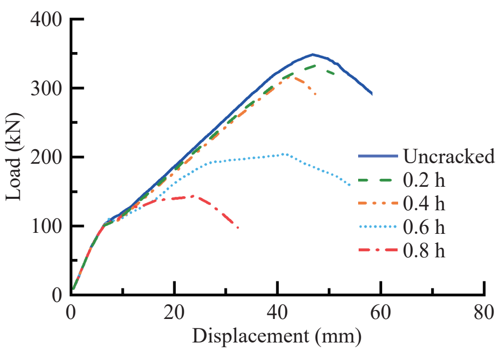

Fig. 11 Load displacement curves (shear crack)

As shown in Figure 12, in the case where only shear cracks are present, the structural cracking pattern and steel reinforcement stress distribution are depicted. It can be observed that in the event of brittle failure, the bottom and top longitudinal reinforcements in the beam structure do not reach the yield state. The structural performance is not fully utilized, but the structure has already experienced failure.

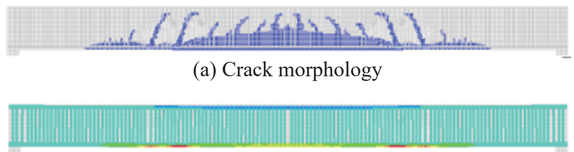

(a) Crack morphology

(b) Reinforcement stress, hoop stress

Fig. 12 Cracks and reinforcement stress diagram (shear crack)

5 Bearing capacity degradation analyses

5.1 Calculation of bending stiffness degradation

As shown in Figure 13, after the concrete simply supported beam cracks, the cracking stiffness of each segment of the beam can be analyzed in segments[7]. Where, B is the full-section flexural stiffness, and B_{cr} is the damaged stiffness after cracking.

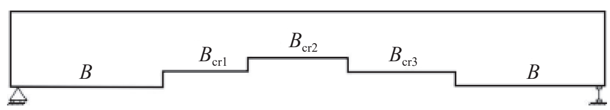

Fig. 13 Stiffness variation diagram of each section of the beam

Based on the load-displacement curve, it is evident that as the load gradually increases, the deformation of the concrete structure, once it incurs damage after cracking, cannot fully recover during the elastic-plastic and plastic phases[17]. The stiffness of various sections can be analyzed based on the load-displacement curve characteristic. When the load-displacement curve is in the elastic phase, the tangent stiffness at this point represents the initial flexural stiffness of the concrete structure. As it enters the elastic-plastic phase and unloads, some of the elastic deformation is recovered, and the stiffness at this point can be obtained as the post-cracking flexural stiffness. This allows us to determine the stiffness reduction pattern. Therefore, when analyzing section damage, it is possible to reflect the trend of section stiffness degradation by analyzing section deformation, thus analyzing the flexural stiffness reduction pattern of the concrete main beam.

The damaged stiffness of concrete beam structures is related to the extent of damage, indicating that crack parameters are linked to structural stiffness after cracking[6,18]. To ensure the generalizability of the results, here, we calculate and analyze the average crack height $\overline{h_{cr}}$ and crack width δ_{cr} following the research conducted by previous scholars.

$$\overline{h_{cr}} = \frac{\sum_{i=1}^{n} h_{cri}}{n}, \tag{3}$$

$$\delta_{cr} = \sum_{i=1}^{n} \delta_{cri}, \tag{4}$$

$$l_{cr} = \sum_{i=1}^{n-1} l_{cri}, \tag{5}$$

$$\overline{\varepsilon_{cr}} = \frac{\delta_{cr}}{l_{cr}}, \tag{6}$$

$$\varphi = \frac{\overline{h_{cr}}}{\overline{\varepsilon_{cr}}}. \tag{7}$$

where, h_{cri} is the height of cracks; δ_{cri} is the crack width; l_{cri} is the extent of cracking; $\overline{\varepsilon_{cr}}$ is strain; φ is curvature.

From the relationship between curvature and deflection can find out the actual value of deflection produced ω_i by each section of the beam under the action of the load, Flexural deformation by elastic deformation ω_α and plastic deformation ω_β Composition. The loss of stiffness can be described in terms of the degree of plasticity to obtain the stiffness reduction relation β_i, The actual bearing capacity M_s can then be brought into the code.

$$\omega_i = \sum_{i=0}^{n} \int_{x_i}^{x_{i+1}} \int_{x_i}^{x_{i+1}} \varphi_i \mathrm{d}x\mathrm{d}x = \omega_\alpha + \omega_\beta (0 \leqslant x_i \leqslant l), \tag{8}$$

$$\beta_i = \frac{B_{cri}}{B} = \frac{\omega_i}{\omega_i + \omega_\beta}. \tag{9}$$

5.2 Calculation of bearing capacity after cracking

According to the specifications (JCT3362—2018), the cracking stiffness of reinforced concrete and prestressed concrete flexural members can be calculated using established structural mechanics methods[19]. The calculation formula is as shown in Equation (10).

$$B = \frac{B_0}{\left(\frac{M_{cr}}{M_s}\right)^2 + \left[1 - \left(\frac{M_{cr}}{M_s}\right)^2\right]\frac{B_0}{B_{cr}}}, \tag{10}$$

where, B is the flexural stiffness of the equivalent section of the cracked member; B_0 is the flexural rigidity of the full section, $B_0 = 0.95E_cI_0$; B_{cr} is the flexural rigidity of the cracked interface, $B_{cr} = E_cI_{cr}$; M_s is the calculation of bending moments by combination of actions; M_{cr} is the cracking bending moment.

Substituting the stiffness reduction factor obtained in the previous Equation (9) into the calculation formula for bending members in (JCT3362—2018), you can derive the formula relating the stiffness reduction factor to the member's load-bearing moment, as shown in Equation (11).

$$M_s = M_{cr}\sqrt{\frac{\beta_i (B_{cr} - B_0)}{B_{cr} - \beta_i B_0}}. \tag{11}$$

The analysis in this paper was conducted on the bridge structure, and a similar method was applied to calculate the mid-span bending moments for two additional bridges on national and provincial highways in the Shanxi region. The calculated results are presented in Table 4 for comparison.

Table 4 Comparison of bending moment values at mid span sections

Method	numerical analysis (kN·m)	Reduction calculation (kN·m)	Deviation (%)
Bridge in this article	2 815.82	2 690.12	4.57
WU YI Bridge	3 521.34	3 416.37	2.98
CHENG BE HE ZHONG Bridge (kN·m)	3 424.74	3 289.46	3.95

Due to the unique characteristics of concrete material properties and the complexities introduced by long-term loading and post-cracking behavior, there is inherent error associated with the analysis when compared to idealized homogeneous material assumptions in concrete structures.

6 Conclusions

Building upon the work of previous scholars, this study investigates the influence of bending cracks and shear cracks on the failure modes of concrete beam structures. Additionally, it explores the reduction patterns in stiffness after cracking. The following conclusions can be drawn.

(1) The presence of bending cracks in concrete bridge structures has a relatively minor impact on the failure modes of the structure. During failure, the structure does not undergo sudden and catastrophic failure but rather

exhibits a certain degree of deformation capacity.

(2) The presence of shear cracks in concrete bridge structures has a significant impact on the failure modes of the structure. With an increase in shear crack height, the structural strength decreases rapidly, leading to brittle failure of the structure. This results in limited deformation capacity and poses a greater risk to the structure.

(3) Building on previous research, this study analyzes the reduction patterns in stiffness after concrete structure damage. It uses post-damage deformation to reflect stiffness reduction and proposes a formula for calculating stiffness reduction coefficients. This formula can be used to assess damage stiffness to some extent.

(4) By using the stiffness reduction formula and applying it to calculate the mid-span sectional bending moment based on (JCT3362—2018), it was observed that the deviation is within 5%. This simplifies the calculation process and provides a method for estimating the residual load-bearing capacity of concrete bridge structures after cracking.

Declaration of competing interest

The author(s) declared no potential conflicts of interest with respect to the research, authorship, and/or publication of this article.

Acknowledgements

This work was supported in part by Shanxi Transportation Holding Group Co., Ltd. project (2022-JKKJ-16); Shanxi Provincial Department of Transportation project (2022-123).

References

[1] Morcos, S.S. Fracture modeling of concrete and steel[J]. Journal of Structural Engineering, 1995, 121(7): 1125–1133.

[2] Castel, A., Vidal, T., Francois, R. Finite-element modeling to calculate the overall stiffness of cracked reinforced concrete beams[J]. Journal of Structural Engineering, 2012, 138(7): 889–898.

[3] Ismail, Z., Kuan, K.K., Yee, K.S., et al. Examining the trend in loss of flexural stiffness of simply supported RC beams with various crack severity using model updating[J]. Measurement, 2014, 50: 43–49.

[4] Benakli, S., Bouafia, Y., Oudjene, M., et al. A simplified and fast computational finite element model for the nonlinear load-displacement behavior of reinforced concrete structures[J]. Composite Structures, 2018, 194(15): 468–477.

[5] Zhao, Y., Zhou, B., He, S.H., et al. Damage stiffness assessment method based on fracture characteristics of PC simply-supported beam[J]. Journal of Chang'an University (Natural Science Edition), 2011, 31(4): 39–44.

[6] Liang, P., Wang, X.L., Lou, C.H., et al. Rapid evaluation of load-bearing capacity of concrete beam bridge based on crack feature library[J]. China Journal of Highway and Transport, 2014, 27(8): 32–41,72.

[7] Wang, L.B., Zhao, Y. Analysis of residual bearing capacity of cracked prestressed concrete continuous box bridges[J]. Journal of Railway Science and Engineering, 2015, 12(1): 127–131.

[8] Li, Y.J., Wu, X.G., Huang, C., et al. Calculation of transverse load distribution coefficient of assembled girder bridge considering main girder damage[J]. Journal of Railway Science and Engineering, 2019, 16(6): 1459–1465.

[9] Zhu, J.L., Wang, P., Chen, B. Model test study on characteristic parameters evolution of prestressed T beams with multiple cracks[J]. Technology of Highway and Transport, 2021, 37(6): 66–72.

[10] JTG D60 —2015, General code for design of highway bridges and culverts[S].

[11] JTG/T H21 —2011, Standard for evaluation of technical conditions of highway bridges[S].

[12] Vecchio, J.F., Shim, W. Experimental and analytical reexamination of classic concrete beam tests[J]. Journal of Structural Engineering, 2004, 130(3): 460–469.

[13] Li, Y., He, S.H., Yan, L. Stiffness degradation analysis on existing bridge with web cracks[J]. Journal of Wuhan University of Technology, 2018, 40(2): 79–83.

[14] Sui, Y., Cheng, X.H., Zhao, Z.Z. Research on cracking failure process of concrete components using total strain crack constitutive model[J]. Journal of Building Structures, 2023, 44(7): 216–224.

[15] Feng, Q., Wu, X.G. Effect of crack statistical parameters of pc bridge on structure[J]. Journal of Highway and Transportation Research and Development, 2017, 34(2): 88–92.

[16] Wang, J.H., Shi, Z.H., Nakano, M. Strength degradation analysis of an aging RC girder bridge using FE crack analysis and simple capacity-evaluation equations[J]. Engineering Fracture Mechanics, 2013, 108: 209–221.

[17] Yu, Z.N., He, S.H., Ren, L.P., et al. Research on residual bearing capacity calculation method and changing law of damaged prestressed concrete box girder[J]. China Journal of Highway and Transport, 2021, 34(9): 242–252.

[18] Zhou, Y.J., Zhao, Y., Zhou, Y., et al. Full-scale experiment on stiffness degradation and identification of prestressed concrete box girders[J]. China Journal of Highway and Transport, 2020, 33(3): 107–118.

[19] JCT3362 —2018, Code for design of highway reinforced concrete and prestressed concrete bridges and culverts[S].